Downloaded from orbit.dtu.dk on: Apr 28, 2024

DTU Library

The Metric of Colour Space

Gravesen, Jens

Published in:
Graphical Models

Link to article, DOI:
10.1016/j.gmod.2015.06.005

Publication date:
2015

Document Version
Peer reviewed version

Link back to DTU Orbit

Citation (APA):
Gravesen, J. (2015). The Metric of Colour Space. *Graphical Models*, *82*(November), 77-86. https://doi.org/10.1016/j.gmod.2015.06.005

General rights
Copyright and moral rights for the publications made accessible in the public portal are retained by the authors and/or other copyright owners and it is a condition of accessing publications that users recognise and abide by the legal requirements associated with these rights.

- Users may download and print one copy of any publication from the public portal for the purpose of private study or research.
- You may not further distribute the material or use it for any profit-making activity or commercial gain
- You may freely distribute the URL identifying the publication in the public portal

If you believe that this document breaches copyright please contact us providing details, and we will remove access to the work immediately and investigate your claim.

The Metric of Colour Space

Jens Gravesen*

May 5, 2015

Abstract

The space of colours is a fascinating space. It is a real vector space, but no matter what inner product you put on the space the resulting Euclidean distance does not corresponds to human perception of difference between colours.

In 1942 MacAdam performed the first experiments on colour matching and found the MacAdam ellipses which are often interpreted as defining the metric tensor at their centres. An important question is whether it is possible to define colour coordinates such that the Euclidean distance in these coordinates correspond to human perception.

Using cubic splines to represent the colour coordinates and an optimisation approach we find new colour coordinates that make the MacAdam ellipses closer to uniform circles than the existing standards.

1 Introduction and background

The human retina has three types of colour photo receptor cone cells, with different spectral sensitivities, see Figure 1, resulting in trichromatic colour vision, i.e., a colour is described by three real numbers. A fourth type of photo receptor cells, the rod, is also present, but they is only used at extremely low light levels (night vision), and does not contribute to the perception of colour. The sensitivities of the colour receptors are not the same for all humans. It depends on the angle under which the colour is observed, but also on age and gender and there are individual variations. Furthermore the perception of colour depends not only on the stimuli of the colour receptors, but also on the environment. The spectral distribution of light reflected from a piece of paper will depend on the light that hits the paper. So if we compare daylight in the morning, daylight at noon, and indoor lightning we get very different spectral distribution, but we will in all cases perceive the reflected light as the same white colour. There are also memory effects: if you watch a colour image which is instantaneously replaced with a grey image you will for a short while perceive not the grey

*email: jgra@dtu.dk, phone: +45 4525 3064

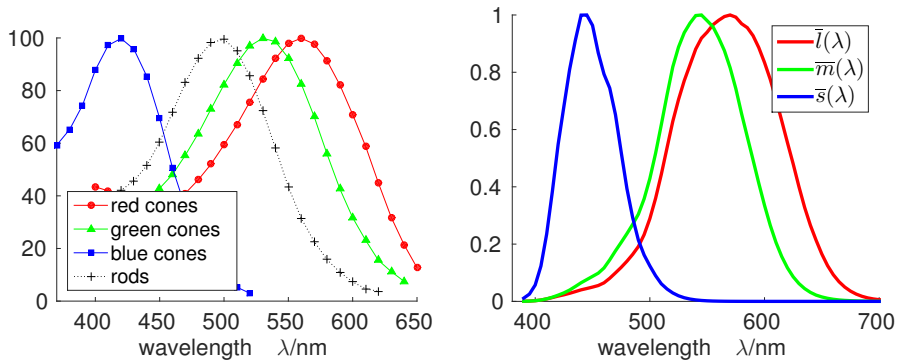

Figure 1: To the left the normalised absorbance spectra of the four human photo receptors, [6]. To the right the normalised sensitivity of the three colour receptors of the human eye, according to the CIE 2006 physiological model, [5], (age 32, angle 2°).

image, but a colour image image consisting of the complementary colours. So there is more to colour perception than the light that hits the eye. We will not consider this very complicated processing done by the brain, but only consider the results of colour perception experiments that have been conducted under very controlled conditions.

In an experiment in 1942 MacAdam discovered that human perception of distance between colours does not correspond to any Euclidean distance in colour space, [9]. These experiments have been repeated and extended many times, see [12]. The results of the experiments are reported as ellipses in 2D and ellipsoids in 3D that can be interpreted as geodesic spheres of a fixed radius. There have since been many attempts to find a distance on colour space that corresponds to human perception. One way is to define new coordinates on colour space such that the Euclidean distance between these coordinates corresponds better to human perception. Most noticeable are the CIE76 standard using the CIE Luv or Lab coordinates, [12], the CIE94 standard using the CIE LCh coordinates, [3], and latest the CIEDE2000 standard, [4, 11]. The CMC l:c standard (1984) also used LCh coordinates; it is a British Standard (BS 6923:1988).

The definition and parametrisation of colour space is an old problem that has attracted interest from many scientists, including names such as Helmholtz and Schrödinger. A recent paper [8] uses a grid optimisation approach to find colour spaces with better perceptual uniformity. Besides perceptual uniformity it is also required that the colour attributes lightness, chroma, and hue are easily obtained. Another difference is that they want the Euclidean distance between colours to agree with the standardised colour-difference formulas above, while we want to improve on those.

In Section 2 we present the basic terminology and colour theory, in par-

ticular the classic colour coordinates. In Section 3 we present the problem of defining a colour difference and describe some existing standards.

In Section 4 we present a method that only focuses on perceptual uniformity and gives us good coordinates on colour space. We consider colour space as a Riemannian manifold and perfect coordinates would give an isometry to Euclidean space. Due to lack of data in electronic form we will only consider MacAdam's original results. MacAdam's experiments took place in a two dimensional slice of colour space so we will only consider the 2D case where luminance is constant. The procedure is a simple two stage process:

1. We identify the MacAdam ellipses with a metric at each of their centres and extend those to a Riemannian metric on all of colour space.

2. We determine a near isometry to Euclidean space $\mathbb{R}^2$.

We use cubic B-splines to represent both the Riemannian metric and the map to $\mathbb{R}^2$ and the two steps can be performed by solving a quadratic optimisation problem. Even though we only consider the 2D case the method is general and can be extended to full 3D colour space.

The result of this process depends on how well the chosen splines can approximate the solution to the two optimisation problems. We expect better results if we increase the degree and/or refine the knot vectors. In this work we have used cubic splines and refined the knot vector until a further refinement did not change the result noticeably. We expect the cubic spline to be close to the true optimum and that we will not obtain any significant improvement by raising the degree of the splines.

Step one is the crucial step. As soon as the Riemannian metric is chosen the best near isometry is essentially fixed. The only freedom left is how to measure the distance from being an isometry. We have used some kind of L^2 distance, but one could of course also use L^1, L^∞, or other distances.

In step one we have chosen the interpolant by simply minimising the second derivative of the components of the logarithm of the metric tensor. This leads to a quadratic optimisation problem but perhaps it would be better to minimise the second derivative of the components of the metric tensor. It would also be possible to consider the curvature of the space and ask for it to be as constant as possible or perhaps as close to zero as possible. Determining the best approach requires more research, should be done using all the available data, not just the classical MacAdam's ellipses, and ideally in colaboration with colour scientists.

One can argue that the MacAdam's ellipses do not determine the metric at their centres but rather are the geodesic unit circles. This point of view leads to a novel geometric question, namely to what extent the unit spheres of a Riemannian manifold determine the metric. We make this precise in Section 6. We finally conclude in Section 7.

2 Colour Space

The International Commission on Illumination, (CIE[1]) has defined several parametrisations of the space of colours, but the starting point and the coordinates in which most experiments are reported are the *CIE XYZ components*. If $I : [\lambda_1, \lambda_2] \to \mathbb{R}_+$ is the intensity function for the light, then the CIE XYZ components are defined by

$$(X, Y, Z) = k \int_{\lambda_1}^{\lambda_2} I(\lambda) \left(\overline{x}(\lambda), \overline{y}(\lambda), \overline{z}(\lambda)\right) \mathrm{d}\lambda \,, \tag{1}$$

where the functions $\overline{x}(\lambda)$, $\overline{y}(\lambda)$, and $\overline{z}(\lambda)$ are the CIE 1931 Standard Colourimetric Observers, see Figure 2, and k is a normalisation constant which

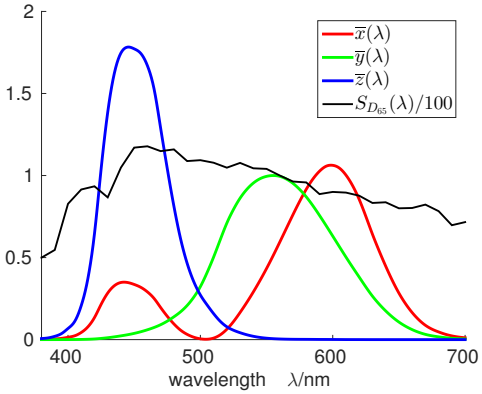

Figure 2: CIE 1931 Standard Colourimetric Observers and the spectral distribution for the CIE illuminant D_{65}. They are tabulated in [12] and can also be found at the CIE web-site [2].

makes $Y = 100$ for a standard light source $S(\lambda)$, i.e.,

$$k = \frac{100}{\int_{\lambda_1}^{\lambda_2} S(\lambda)\, \overline{y}(\lambda)\, \mathrm{d}\lambda} \,. \tag{2}$$

For the CIE standard illuminant D_{65}, see Figure 2, we have $k = 0.047332$. The number Y is called the *luminance* and is an attempt to define the total observed intensity of the light.

The colour of an object depends on the light that hits the object and how the object reflects light of a given wavelength. The observed colour stimuli is given as

$$(X, Y, Z) = k \int_{\lambda_1}^{\lambda_2} I(\lambda)\, \rho(\lambda) \left(\overline{x}(\lambda), \overline{y}(\lambda), \overline{z}(\lambda)\right) \mathrm{d}\lambda \,, \tag{3}$$

[1] `http://www.cie.co.at`

where $\rho(\lambda) \in [0,1]$ is the spectral reflectance of the object. The possible colour stimuli that can be obtained, when the incident light is some standard light source such as D_{65}, are convex combinations of *optimal colour stimuli*, i.e., light reflected from objects whose spectral reflectance $\rho(\lambda) \in \{0,1\}$ is either constant zero except in an interval $[\lambda_1, \lambda_2]$ where it is one, type 1, or vice verse for type 2, see Figure 3. The width of the interval $[\lambda_1, \lambda_2]$

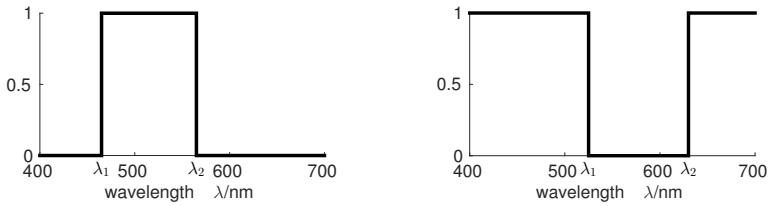

Figure 3: Spectral reluctance curves for the two types of optimal colour stimuli. Type 1 to the left and type 2 to the right.

is chosen such that luminance Y is some given value, normally given as a percentage of the luminance of the illuminant.

Ideally we would like the eye sensitivities $(\bar{l}, \overline{m}, \overline{s})$ to be a linear combination of $(\overline{x}, \overline{y}, \overline{z})$, but this is not the case. Indeed, if we determine a 3×3 matrix $\mathbf{C}$ in the least square sense such that $(\bar{l}, \overline{m}, \overline{s})^T = \mathbf{C}\,(\overline{x}, \overline{y}, \overline{z})^T$, then we obtain

$$\begin{pmatrix} \bar{l} \\ \overline{m} \\ \overline{s} \end{pmatrix} \approx \begin{pmatrix} 0.2684 & 0.8466 & -0.0349 \\ -0.3869 & 1.1681 & 0.1031 \\ 0.0214 & -0.0247 & 0.5388 \end{pmatrix} \begin{pmatrix} \overline{x} \\ \overline{y} \\ \overline{z} \end{pmatrix}, \tag{4}$$

and, as we can see in Figure 4, we do not have a strict equality.

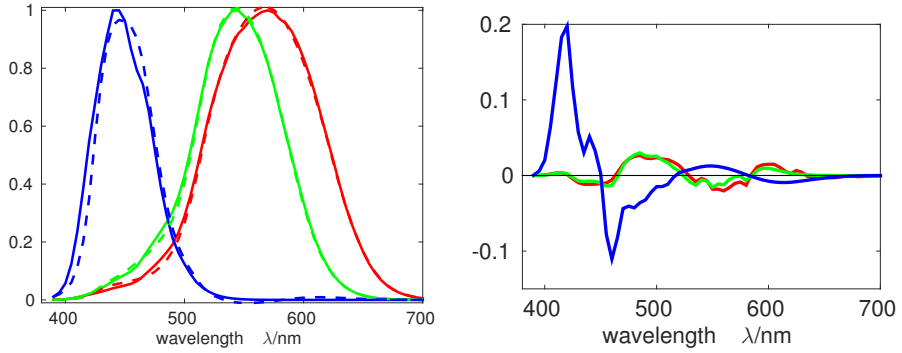

Figure 4: To the left $(\bar{l}, \overline{m}, \overline{s})$ in solid lines and $\mathbf{C}\,(\overline{x}, \overline{y}, \overline{z})^T$ in dashed lines. To the right the difference.

The *CIE xy chromatic coordinates* are given by

$$x = \frac{X}{X+Y+Z}, \qquad y = \frac{Y}{X+Y+Z}. \tag{5}$$

Sometimes a third coordinate $z = Z/(X+Y+Z)$ is defined, but it can always be found from the relation $x + y + z = 1$. The two chromatic coordinates x and y describe "pure" colour, in the absence of luminance (or brightness). When monochromatic light sweeps over the visual light range from 400nm to 700nm, it traces a curve in the xy-space, see Figure 5. The line connecting

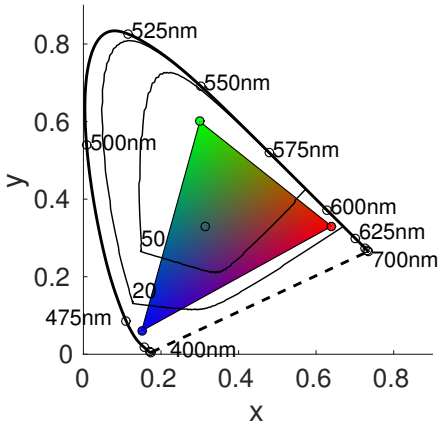

Figure 5: The tristimulus diagram. The monochromatic colours lie on the curved part of the boundary. The dashed line joining the the end of the visible spectrum [380nm, 700nm] is the line of purples. The triangle contain the colours that can be produced by the primaries of the Rec. 709 RGB specifications (HDTV), [1]. The circle indicates the D_{65} white point and the two inner curves are the optimal colour stimuli for the D_{65} illuminant at 20% and 50%, respectively.

the two ends of the curve is called the line of purples. It joins extreme blue with extreme red and consists consequently of mixtures of blue and red.

A colour can be specified by chromaticity (x, y) and luminance Y in the form of the *CIE xyY components*. To recover X and Z the following formulae are used:

$$X = Y\,\frac{x}{y}\,, \qquad Z = Y\,\frac{1-x-y}{y}\,. \tag{6}$$

The colours on a computer screen or a television are given by mixing three *primaries*: red, green, and blue. The three primaries correspond to three points in xy-space and the screen can reproduce all colours in the triangle spanned by the three primaries, the *gamut* of the primaries. In Figure 5 the primaries for the HDTV, [1], are plotted and it is easily seen that not all colours can be obtained. The actual colours in the plot need not be correct, they depend on the computer screen, or on the printer and the illumination. Other devices such as a computer screen, a projector, etc. also have three primary colours and can only reproduce the colours in some triangle.

2.1 Uniform CIE colour spaces

The *CIE Luv coordinates* (1976), [12] is an attempt to create a perceptually uniform colour space and the components are given by

$$L^* = \begin{cases} 903.3\, Y/Y_n & \text{if } Y/Y_n \le 0.008856\,, \\ 116\, \sqrt[3]{Y/Y_n} - 16 & \text{if } Y/Y_n > 0.008856\,, \end{cases} \tag{7}$$

$$u^* = 13L^*(u' - u'_n)\,, \tag{8}$$

$$v^* = 13L^*(v' - v'_n)\,. \tag{9}$$

The quantities u', v', u'_n, and v'_n are given by

$$u' = \frac{4X}{X + 15Y + 3Z}\,, \qquad u'_n = \frac{4X_n}{X_n + 15Y_n + 3Z_n}\,, \tag{10}$$

$$v' = \frac{9Y}{X + 15Y + 3Z}\,, \qquad v'_n = \frac{9Y_n}{X + 15Y_n + 3Z_n}\,. \tag{11}$$

The triple (X_n, Y_n, Z_n) defines the origin in the u^*v^*-plane and consists of the components of the white reference, where Y_n is normalised to 100. For the D_{65} white point the values are $(X_n, Y_n, Z_n) = (95.043, 100, 108.88)$.

In the *CIE Lab coordinates* (1976) the components (u^*, v^*) are replaced by (a^*, b^*) that are given by

$$a^* = 500\big(f(X/X_n) - f(Y/Y_n)\big)\,, \tag{12}$$

$$b^* = 200\big(f(Y/Y_n) - f(Z/Z_n)\big)\,, \tag{13}$$

where

$$f(t) = \begin{cases} 7.787\, t + 16/116 & \text{if } t \le 0.008856\,, \\ \sqrt[3]{t} & \text{if } t > 0.008856\,. \end{cases} \tag{14}$$

In the *CIE Lch coordinates* the Cartesian coordinates (a^*, b^*) are replaced by polar coordinates (c, h) called *chroma* and *hue* respectively, i.e.,

$$a^* = c\cos h\,, \qquad b^* = c\sin h\,. \tag{15}$$

3 Colour Differences

The human perception of similar colours has not much to do with the Euclidean distance in the xy-plane. Indeed, some sixty years ago MacAdam conducted some colour matching experiments where a person was asked to match a colour with given chromatic coordinates (x, y) by adjusting another colour by a single control that traced a line through (x, y) in the chromatic plane. The standard deviations were approximately ellipses in the chromatic plane, see Figure 6. In [12, Table 2(5.4.1)] we can find the centres $\mathbf{x}_k = (x_k, y_k) \in [0, 1]^2$ and values a_k, b_k, θ_k of the major axis, the minor axis

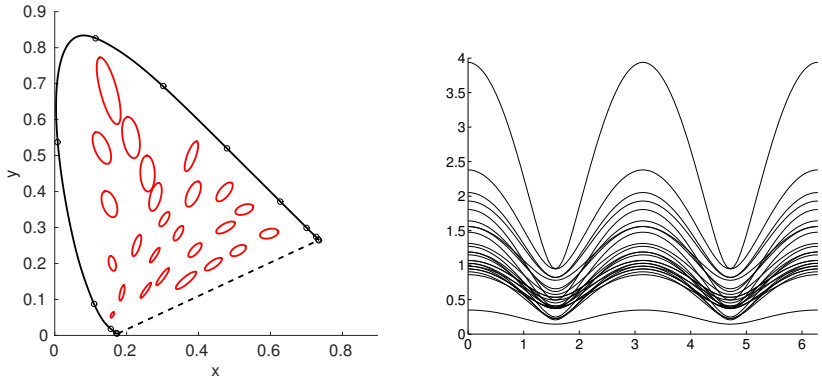

Figure 6: To the left the 25 MacAdam ellipses, [9], enlarged 10 times. If the depicted ellipses are scaled by 0.3 then colours on the ellipse can just be seen to be different from the colour at the centre. To the right the normalised distance along the MacAdam ellipses from their centre.

and the angle of the major axis of the 25 MacAdam ellipses, respectively. That is, the kth ellipse can be parametrised as

$$\mathbf{x}_k(\theta) = (x_k(\theta), y_k(\theta)) = (x_k, y_k) + (a\cos(\theta+\theta_k), b\,\sin(\theta+\theta_k))\,. \tag{16}$$

To the right in Figure 6 we have illustrated the deviation from circles of the same size by plotting the normalised distance from the centre. The normalisation is done by requiring that the total average distance should be one. That is we plot

$$d_k(\theta) = \frac{\|\mathbf{x}_k(\theta) - \mathbf{x}_k\|}{\frac{1}{25}\sum_{\ell=1}^{25}\frac{1}{2\pi}\int_0^{2\pi}\|\mathbf{x}_\ell(\theta)-\mathbf{x}_\ell\|\,\mathrm{d}\theta}\,. \tag{17}$$

In Table 1 we have listed the deviation from the unit circle in the L^2-norm

$$\|d_k - 1\|_2 = \sqrt{\frac{1}{2\pi}\int_0^{2\pi}(d_k(\theta)-1)^2\,\mathrm{d}\theta}\,, \tag{18}$$

for this and several other colour differences.

If the ellipses are enlarged approximately three times they define the *just noticeable difference*, i.e., colours inside the enlarged ellipse appear to be the same as the one at the centre while colours outside appear to be different from the colour at the centre. This discrepancy between human perception and the Euclidean distance has spawned several attempts to define parameters which are more uniform with respect to the human perception.

MacAdam's experiments have been repeated and also extended to include intensity so we have ellipsoids in the $xy\ell$ colour space, where $\ell =$

$0.2\log_{10}(Y)$, see [12, Tables I and II(5.4.2), and I(5.4.3–4)]. We don't have the 3D results in electronic form so all numerical experiments are done using the MacAdam ellipses in the 2D xy colour space.

The CIE Luv coordinates are meant to define perceptually uniform colour space and the images of the MacAdam ellipses do have a more uniform size, but their shapes are far from circular, see Figure 7. The colour

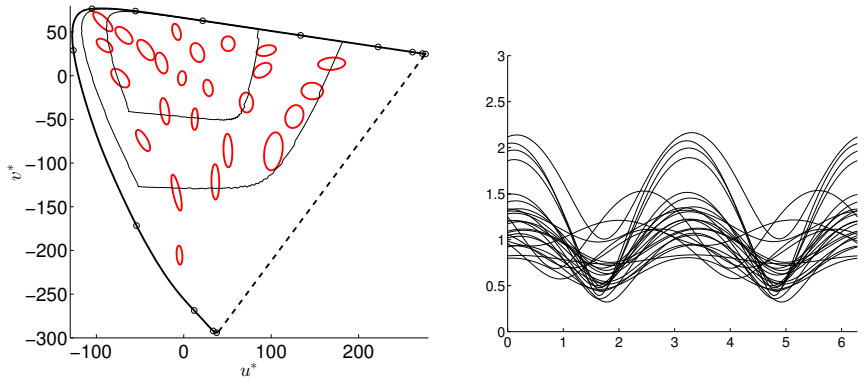

Figure 7: To the left the image of the MacAdam ellipses in the u^*v^*-plane. To the right the normalised distances along the ellipses from their centres.

distance ΔE^*_{uv}, between two colours is simply the Euclidean distance, i.e.,

$$\Delta {E^*_{uv}}^2 = \Delta u^{*2} + \Delta v^{*2} + \Delta L^{*2}\,. \tag{19}$$

The CIE Lab coordinates are also meant to define perceptually uniform colour space, see Figure 8. The colour distance, called CIE76, is again the

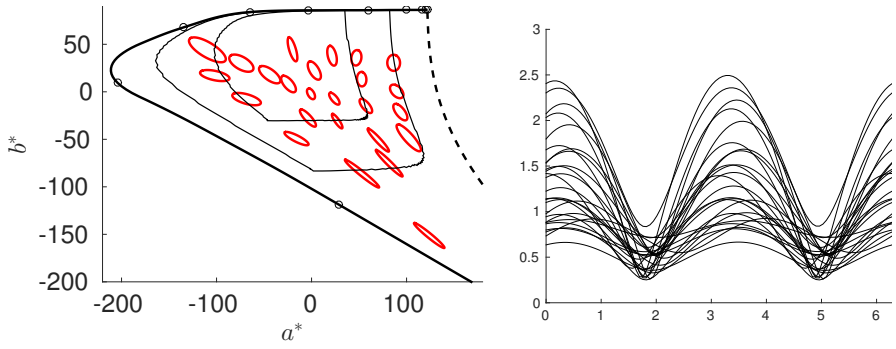

Figure 8: To the left the image of the MacAdam ellipses in the a^*b^*-plane. To the right the normalised distances along the ellipses from their centres.

Euclidean distance

$$\Delta {E^*_{ab}}^2 = \Delta a^{*2} + \Delta b^{*2} + \Delta L^{*2}\,. \tag{20}$$

The CIE94 colour distance ΔE_{ch} uses the polar coordinates croma and hue (15) and the distance between the colours (L_1^*, c_1, h_1) and (L_2^*, c_2, h_2) is defined by

$$\Delta {E_{ch}}^2 = \left(\frac{\Delta L^*}{K_L\, S_L}\right)^2 + \left(\frac{\Delta c}{K_c\, S_c}\right)^2 + \left(\frac{\Delta h}{K_h\, S_h}\right)^2 , \tag{21}$$

where Δh is defined such that

$$\Delta c^2 + \Delta h^2 = \Delta {a^*}^2 + \Delta {b^*}^2 , \tag{22}$$

i.e.,

$$\Delta {E_{ch}}^2 = \left(\frac{\Delta L^*}{K_L\, S_L}\right)^2 + \left(\frac{\Delta c}{K_c\, S_c}\right)^2 + \frac{\Delta {a^*}^2 + \Delta {b^*}^2 - \Delta c^2}{(K_h\, S_h)^2} . \tag{23}$$

The terms in the denominator depend on the application. In the case of graphic arts they are

$$S_L = 1 , \qquad S_c = 1 + 0.045\, c_1 , \qquad S_h = 0.015\, c_1 , \tag{24}$$

$$K_L = 1 , \qquad K_c = 1 , \qquad K_h = 1 . \tag{25}$$

Observe that the distance is asymmetric. In Figure 9 we have plotted the

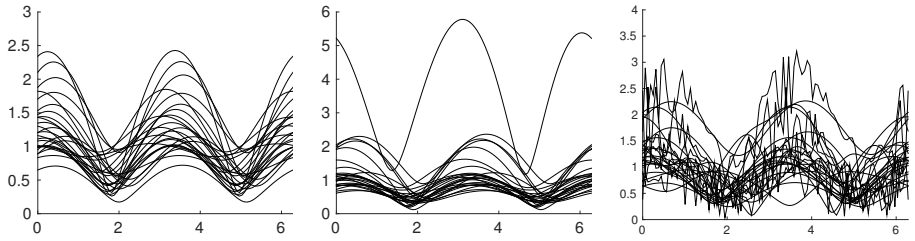

Figure 9: To the left the CIE94 distance (normalised) along the ellipses from their centres. In the centre and to the right, the same using the CMC 2:1 distance and the CIEDE2000 distance, respectively.

distances along the ellipses from their centres according to this definition. The CMC l:c distance (1984) is also based on *Lch* coordinates and is given as follows

$$\Delta {E_{\ell:c}}^2 = \left(\frac{\Delta L^*}{\ell\, S_L}\right)^2 + \left(\frac{\Delta c}{c\, S_c}\right)^2 + \frac{\Delta {a^*}^2 + \Delta {b^*}^2 - \Delta c^2}{(S_h)^2} , \tag{26}$$

where $\ell = 2$ and $c = 1$ are often used and

$$S_L = \begin{cases} 0.511 & L_1^* < 16 , \\ \frac{0.040975\, L*_1}{1+0.01765\, L_1^*} & L_1^* \geq 16 , \end{cases} \tag{27}$$

$$S_C = \frac{0.0638\, c_1}{1 + 0.0131\, c_1} , \tag{28}$$

$$S_h = S_C\, (F\, T + 1 - F) , \tag{29}$$

and

$$F = \sqrt{\frac{c_1^4}{1900 + c_1^4}}\,, \tag{30}$$

$$T = \begin{cases} 0.56 + |0.2\cos(h1 + 168°)| & 164° \le h_1 \le 345°\,, \\ 0.36 + |0.4\cos(h1 + 35°)| & \text{otherwise.} \end{cases} \tag{31}$$

The result is plotted in Figure 9. Again we have an asymmetric distance. We finally look at the CIEDE2000 distance. It too is based on the Lch colour space

$$\Delta {E_{00}}^2 = \left(\frac{\Delta L^*}{k_L\, S_L}\right)^2 + \left(\frac{\Delta C'}{k_C\, S_C}\right)^2 + \left(\frac{\Delta H'}{k_H\, S_H}\right)^2 + R_T \frac{\Delta C'}{k_C\, S_C}\frac{\Delta H'}{k_H\, S_H}\,, \tag{32}$$

where

$$\overline{c} = \frac{c_1 + c_2}{2}\,, \tag{33}$$

$$a_i' = a_i^* + \frac{a_i^*}{2}\left(1 - \sqrt{\frac{\overline{c}^7}{\overline{c}^7 + 25^7}}\right)\,, \tag{34}$$

$$(a_i', b_i^*) = C_i'(\cos h_i', \sin h_i')\,, \quad h_i \in [0, 2\pi[\,, \tag{35}$$

$$\overline{C'} = \frac{C_1' + C_2'}{2}\,, \tag{36}$$

$$\Delta h' = \begin{cases} h_2' - h_1'\,, & |h_2' - h_1'| \le \pi\,, \\ h_2' - h_1' - 2\pi\,, & h_2' - h_1' > \pi\,, \\ h_2' - h_1' + 2\pi\,, & h_2' - h_1' < -\pi\,, \end{cases} \tag{37}$$

$$\Delta H' = 2\sqrt{C_1'\, C_2'}\,\sin\left(\frac{\Delta h'}{2}\right)\,, \tag{38}$$

$$\overline{h'} = \begin{cases} (h_1' + h_2')/2\,, & |h_2' - h_1'| \le \pi\,, \\ (h_1' + h_2' + 2\pi)/2\,, & |h_2' - h_1'| > \pi\,, \quad h_1' + h_2' < 2\pi\,, \\ (h_1' + h_2' - 2\pi)/2\,, & |h_2' - h_1'| > \pi\,, \quad h_1' + h_2' \ge 2\pi\,, \end{cases} \tag{39}$$

$$\begin{aligned} T = {} & 1 - 0.17\cos(\overline{h'} - 30°) + 0.24\cos(2\overline{h'}) \\ & + 0.32\cos(3\overline{h'} + 6°) - 0.20\cos(4\overline{h'} - 63°)\,, \end{aligned} \tag{40}$$

$$\overline{L} = \frac{L_1^* + L_2^*}{2}\,, \tag{41}$$

$$S_L = 1 + \frac{0.015(\overline{L} - 50)^2}{\sqrt{20 + (\overline{L} - 50)^2}}\,, \tag{42}$$

$$S_C = 1 + 0.045\overline{C'}\,, \tag{43}$$

$$S_H = 1 + 0.015\overline{C'}\,T\,, \tag{44}$$

$$R_T = -2\sqrt{\frac{\overline{C'}^7}{\overline{C'}^7 + 25^7}}\,\sin\left(60^\circ\,\exp\left(-\frac{\overline{h'} - 275^\circ}{25^\circ}\right)\right)\,. \tag{45}$$

The result is plotted in Figure 9.

4 New colour coordinates

We define the new coordinates in a two stage process where we first obtain a Riemannian metric on the colour space and then find a near isometry to Euclidean space.

4.1 Extrapolating the MacAdam Ellipses or the Metric

By regarding the MacAdam ellipses as being in the tangent space at the centre $\mathbf{x}_k$ we can identify them with a metric on the tangent space given by

$$\begin{pmatrix} E_k & F_k \\ F_k & G_k \end{pmatrix} = \begin{pmatrix} \cos\theta_k & -\sin\theta_k \\ \sin\theta_k & \cos\theta_k \end{pmatrix} \begin{pmatrix} 1/a_k^2 & 0 \\ 0 & 1/b_k^2 \end{pmatrix} \begin{pmatrix} \cos\theta_k & \sin\theta_k \\ -\sin\theta_k & \cos\theta_k \end{pmatrix}\,. \tag{46}$$

We now extrapolate the components of this metric to the rectangle $\Omega = [0.0, 0, 8] \times [0.0, 0.9]$. In order to keep the matrix positive definite we consider the matrix logarithm

$$\begin{aligned} \begin{pmatrix} e_k & f_k \\ f_k & g_k \end{pmatrix} &= \log \begin{pmatrix} E_k & F_k \\ F_k & G_k \end{pmatrix} \\ &= -2 \begin{pmatrix} \cos\theta_k & -\sin\theta_k \\ \sin\theta_k & \cos\theta_k \end{pmatrix} \begin{pmatrix} \log a_k & 0 \\ 0 & \log b_k \end{pmatrix} \begin{pmatrix} \cos\theta_k & \sin\theta_k \\ -\sin\theta_k & \cos\theta_k \end{pmatrix}\,, \end{aligned} \tag{47}$$

We extrapolate the components to Ω by solving the following linear constrained quadratic optimisation problem:

$$\text{minimise} \int_0^{0.9} \int_0^{0.8} \left|\frac{\partial^2 e}{\partial x^2}\right|^2 + 2\left|\frac{\partial^2 e}{\partial x \partial y}\right|^2 + \left|\frac{\partial^2 e}{\partial y^2}\right|^2 \,\mathrm{d}x\,\mathrm{d}y\,, \tag{48}$$

$$\text{such that } e(x_k, y_k) = e_k, \quad k = 1, \ldots, K\,, \tag{49}$$

and similar for f and g. We use cubic B-splines to represent the functions e, f, and g and `quadprog` from Matlab's Optimisation toolbox [10] to solve the optimisation problem. We find the components of the metric by taking the matrix exponential

$$\begin{pmatrix} E(x,y) & F(x,y) \\ F(x,y) & G(x,y) \end{pmatrix} = \exp \begin{pmatrix} e(x,y) & f(x,y) \\ f(x,y) & g(x,y) \end{pmatrix} \tag{50}$$

the corresponding field of ellipses can be seen in Figure 10 together with the Gaussian curvature. As we can see the Gaussian curvature is not zero so we cannot get a perfect isometry with Euclidean space.

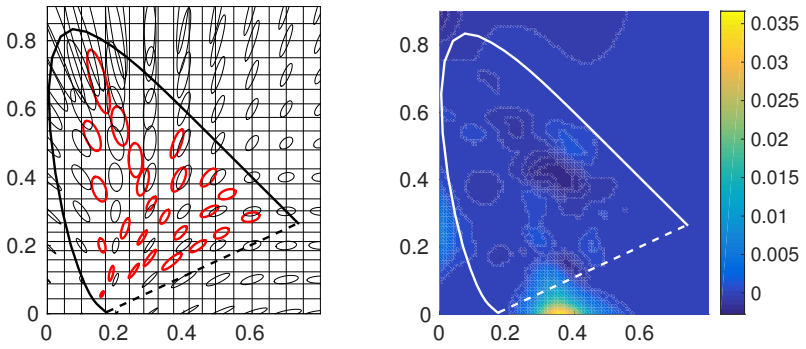

Figure 10: To the left the black ellipses are the result of interpolating (and extrapolating) the metric corresponding to the MacAdam ellipses. The knots are indicated by the thin lines. To the right the Gaussian curvature.

4.2 Obtaining a near isometry to Euclidean space

We seek a map $(\xi, \eta) : \Omega \to \mathbb{R}^2$ such that the Euclidean distance in $\xi\eta$ space is in good agreement with human perception of colour distance. That is, we want the images of the ellipses to be circles of equal size. This is the same as saying that we have an isometry with respect to the extrapolated metric on Ω and the standard Euclidean metric on $\mathbb{R}^2$.

If the major and minor axes of the ellipses, or equivalently the eigenvectors of the metric tensor, map to the standard basis in $\mathbb{R}^2$ then we do have an isometry. The Jacobian of our map is

$$J = \begin{pmatrix} \partial\xi/\partial x & \partial\xi/\partial y \\ \partial\eta/\partial x & \partial\eta/\partial y \end{pmatrix}, \tag{51}$$

the eigenvectors are $(a\,\cos\theta, a\,\sin\theta)$ and $(-b\,\sin\theta, b\,\cos\theta)$, respectively, and they map to the standard basis if

$$J \begin{pmatrix} a\,\cos\theta & -b\,\sin\theta \\ a\,\sin\theta & b\,\cos\theta \end{pmatrix} = \begin{pmatrix} 1 & 0 \\ 0 & 1 \end{pmatrix}, \tag{52}$$

or equivalently

$$J = \begin{pmatrix} a\,\cos\theta & -b\,\sin\theta \\ a\,\sin\theta & b\,\cos\theta \end{pmatrix}^{-1} = \frac{1}{ab} \begin{pmatrix} b\,\cos\theta & b\,\sin\theta \\ -a\,\sin\theta & a\,\cos\theta \end{pmatrix}. \tag{53}$$

We now solve the quadratic optimisation problem

$$\text{minimise} \int_0^{0.9} \int_0^{0.8} \left(\left(\frac{\partial\xi}{\partial x} - \frac{\cos\theta}{a} \right)^2 + \left(\frac{\partial\xi}{\partial y} - \frac{\sin\theta}{a} \right)^2 \right) w \,\mathrm{d}x\,\mathrm{d}y \tag{54}$$

$$\text{such that } \xi(0.1, 0.0) = 0\,, \tag{55}$$

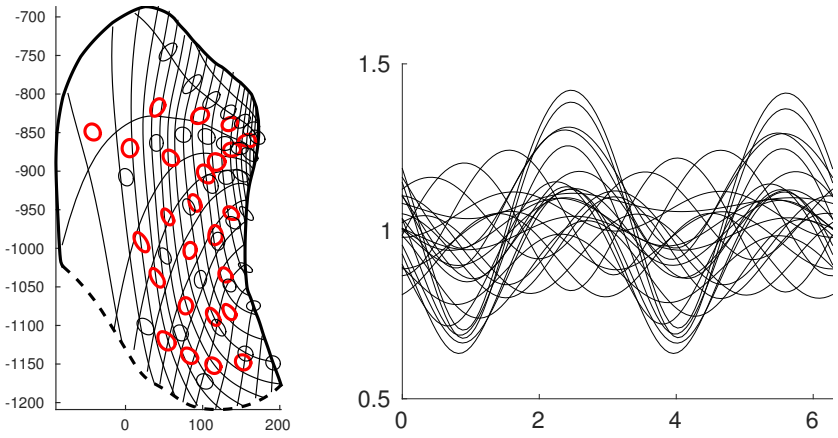

Figure 11: To the left the new colour space obtained by (54). To the right the normalised distances along the ellipses from their centre.

and similar for η, where w is a weight function which is 100 inside the visible colours and 1 outside. Expressing ξ and η using the same B-splines as before and also Matlab's `quadprog` [10], we obtain the result in Figure 11.

The advantage of this approach is that it leads to a quadratic programming problem which has unique solution and is relatively cheap to solve. The disadvantage is that we restrict the set of possible solutions. We ask that the images of the eigenvectors (or semiaxis) map to the standard basis but it is sufficient (and necessary) that they map to an arbitrary orthonormal basis. That is, we have an isometry if

$$J \begin{pmatrix} a\cos\theta & -b\sin\theta \\ a\sin\theta & b\cos\theta \end{pmatrix} = \begin{pmatrix} \cos\phi & -\sin\phi \\ \sin\phi & \cos\phi \end{pmatrix}, \tag{56}$$

for some function ϕ or equivalently

$$J = \begin{pmatrix} \cos\phi & -\sin\phi \\ \sin\phi & \cos\phi \end{pmatrix} \begin{pmatrix} \dfrac{\cos\theta}{a} & \dfrac{\sin\theta}{a} \\ -\dfrac{\sin\theta}{b} & \dfrac{\cos\theta}{b} \end{pmatrix}. \tag{57}$$

That leads us to the following optimisation problem

$$\begin{aligned} \text{minimise} \int_0^{0.9}\int_0^{0.8} \Bigg(\left(\frac{\partial\xi}{\partial x} - \cos\phi\,\frac{\cos\theta}{a} - \sin\phi\,\frac{\sin\theta}{b} \right)^2 + \\ \left(\frac{\partial\xi}{\partial y} - \cos\phi\,\frac{\sin\theta}{a} + \sin\phi\,\frac{\cos\theta}{b} \right)^2 + \left(\frac{\partial\eta}{\partial x} - \sin\phi\,\frac{\cos\theta}{a} + \cos\phi\,\frac{\sin\theta}{b} \right)^2 \\ + \left(\frac{\partial\eta}{\partial y} - \sin\phi\,\frac{\sin\theta}{a} - \cos\phi\,\frac{\cos\theta}{b} \right)^2 \Bigg) w \,\mathrm{d}x\,\mathrm{d}y\,, \end{aligned} \tag{58}$$

such that $(\xi(0.1,0),\eta(0.1,0)) = (0,0)$ and $\phi(0.1,0) = 0$. This is not a quadratic problem and we now use Matlab's `fmincon` [10] to solve the optimisation problem. The result is shown in Figure 12.

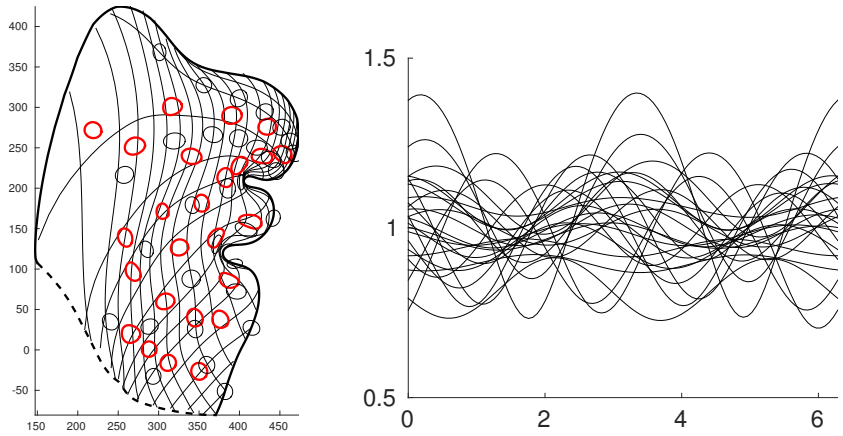

Figure 12: To the left the new colour space obtained by (58). To the right the normalised distances along the ellipses from their centre.

A warning is wareanted here. There is nothing that guaranties that the optimisations (54) and (58) give an injective map $(\xi,\eta):\Omega\to\mathbb{R}^2$. Indeed if we use a coarse spline space then (58) yields a non injective map. This can be circumvented by adding $\det J > 0$ as a constraint in the optimisation. Here it is crucial to express $\det J$ in B-spline form, see [7, Theorem 1].

It should also be noted that we have assumed that the axes of the MacAdam ellipses $(a\,\cos\theta, a\,\sin\theta)$ form a smooth vector field, i.e., we chose the eigenvectors of the metric (50) such that they form smooth vector fields. This can always be done, but could be cumbersome. Alternatively we could use that our map is an isometry if and only if

$$J^T J = \begin{pmatrix} \xi_x^2+\eta_x^2 & \xi_x\,\xi_y+\eta_x\,\eta_y \\ \xi_x\,\xi_y+\eta_x\,\eta_y & \xi_y^2+\eta_y^2 \end{pmatrix} = \begin{pmatrix} E & F \\ F & G \end{pmatrix}, \tag{59}$$

where ξ_x, ξ_y, η_x, and η_y denotes the partial derivatives. This would give us the following optimisation problem

$$\text{minimise} \int_0^{0.9}\int_0^{0.8} \left(\xi_x^2+\eta_x^2-E\right)^2 + 2\left(\xi_x\,\xi_y+\eta_x\,\eta_y-F\right)^2 + \left(\xi_x^2+\eta_x^2-G\right)^2 \,\mathrm{d}x\,\mathrm{d}y\,. \tag{60}$$

5 Results

The results are summarised in Table 1 where we have listed how much the

i	xy	uv	ab	CIE94	CMC	CIE00	new 1	new 2
1	7.49	3.61	7.81	5.47	4.82	5.23	0.58	0.37
2	4.48	6.83	9.47	4.30	4.05	4.09	0.72	1.15
3	4.18	6.32	7.20	3.89	4.17	3.66	2.65	1.02
4	19.84	3.20	8.76	1.33	2.64	3.19	1.14	0.91
5	5.86	2.56	4.43	2.84	3.98	3.31	1.07	0.43
6	9.03	2.12	3.17	0.86	2.73	3.14	0.99	1.65
7	6.68	2.43	2.92	2.72	1.72	4.92	0.81	1.39
8	3.44	2.15	4.29	3.06	2.87	3.62	1.02	0.99
9	4.07	2.20	2.63	5.27	3.75	5.61	1.78	0.91
10	5.18	3.34	3.55	2.41	2.83	2.78	1.47	2.51
11	3.89	2.95	3.93	9.14	6.41	7.40	1.40	0.83
12	3.32	3.62	3.30	8.00	7.78	4.59	0.96	0.96
13	3.70	3.78	4.92	5.09	31.52	8.66	1.60	0.72
14	3.54	1.58	2.56	6.68	8.60	11.51	1.47	1.76
15	2.60	2.19	2.79	4.04	7.42	6.68	1.32	1.54
16	2.58	2.32	2.96	2.62	2.93	3.85	1.84	0.36
17	2.91	1.69	3.38	3.02	3.31	3.87	1.97	0.54
18	2.96	1.25	2.85	3.64	4.89	4.21	0.70	0.61
19	2.58	3.31	1.97	3.18	3.89	3.89	0.35	0.30
20	3.70	2.97	4.33	2.78	2.69	2.74	1.13	0.38
21	3.28	1.41	3.38	3.02	4.14	3.18	0.67	0.73
22	3.20	1.96	2.75	3.62	4.92	3.99	1.16	1.06
23	4.21	3.34	4.14	3.19	3.99	2.84	2.00	1.89
24	3.78	5.63	5.14	3.53	4.14	3.53	2.50	1.45
25	3.75	7.55	6.15	3.08	3.67	3.25	1.82	0.66
avg	4.81	3.21	4.35	3.87	5.35	4.55	1.32	1.00

Table 1: The deviation of the MacAdam's ellipses from the unit circle measured in the L^2 norm, cf. (18). The worst cases are marked with a grey background.

MacAdam's ellipses deviate from the unit circle in the L^2-norm, see (17)and (18), for all the colour differences considered in this paper. As we have defined the distance from the centre of the ellipses to any point on the ellipse to be one it is clearly seen that the Euclidean distance in two new colour spaces are significantly closer to MacAdam's observations than any of the classical colour distances.

6 Mathematical afterthoughts

In the preceding sections we have identified the MacAdam ellipses with a metric on the tangent space at the centre of the ellipses. This is an

approximation; a more correct interpretation of the MacAdam ellipses is to regard them as unit circles. In principle we can find the MacAdam ellipse for any visual colour so we can imagine that we have a field of unit circles in an open subset of the xy-plane. A natural question is now whether there exists a metric which has the given curves as unit circles. We can also specialise the metric to be a Riemannian metric. If such a metric exists then we can ask if it is unique. As the distance from the centre to points on a sphere is the same as the distance from points on the sphere to the centre we have an obvious consistency condition, see Figure 13. By considering geodesic spheres with radius $t \in [0, 1]$ we obtain a contraction of a unit sphere onto its centre.

Definition 1. A field of spheres on an n-dimensional manifold M is a map $M \to C(S^{n-1}, M) : x \mapsto \gamma_x$ such that we for all $x \in M$ have that γ_x is an embedding, $x \notin \gamma_x(S^{n-1})$, and $\gamma_x(S^{n-1})$ contracts onto x. If $x \in \gamma_{\gamma_x(y)}$ for all $x \in M$ and $y \in S^{n-1}$ then we call the field of spheres consistent.

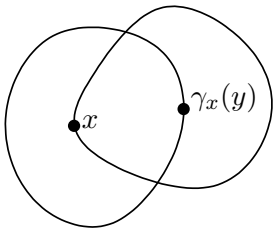

Figure 13: The necessary consistency condition for a field of unit spheres.

Definition 2. If $M \to C(S^{n-1}, M) : x \mapsto \gamma_x$ is a consistent field of spheres on M then a Riemannian metric on M is called compatible if we, for all x, have that $\gamma_x(S^{n-1})$ is the geodesic unit-sphere centred at x.

Question 1. Is there a compatible metric for every consistent field of spheres on a manifold M?

Question 2. Is a metric as in Question 1 unique?

These are natural geometric questions but they have to my knowledge never been studied. The general questions are probably hard, but in dimension one they become almost trivial and we can give a complete answer.

The answer in 1D

A one dimensional manifold is either diffeomorphic to $\mathbb{R}$ or to S^1, and the later case can be reduced to $\mathbb{R}$ by pulling the field of spheres and the metric back to $\mathbb{R}$ by the exponential map $\mathbb{R} \to S^1$.

A field of spheres on $\mathbb{R}$ is simply two maps $a, b : \mathbb{R} \to \mathbb{R}$, such that $a(x) < x < b(x)$, for all $x \in \mathbb{R}$. The consistency condition reads

$$x \in \{a(a(x)), b(a(x))\}\,, \quad \text{and} \quad x \in \{a(b(x)), b(b(x))\}\,. \tag{61}$$

As $a(a(x)) < a(x) < x < b(x) < b(b(x))$ we must have $x = b(a(x))$ and $x = a(b(x))$, i.e.,

$$a = b^{-1}\,, \qquad \text{and hence} \qquad a'(b(s))\, b'(s) = 1\,. \tag{62}$$

A Riemannian metric on $\mathbb{R}$ is simply a weight function $\alpha : \mathbb{R} \to \mathbb{R}_+$ and $\{a(x), b(x)\}$ is a unit sphere centred at x if and only if

$$\int_{a(x)}^{x} \alpha(t)\,\mathrm{d}t = 1\,, \qquad \text{and} \qquad \int_{x}^{b(x)} \alpha(t)\,\mathrm{d}t = 1\,. \tag{63}$$

Differentiation with respect to x yields

$$a'(x)\alpha(a(x)) = \alpha(x)\,, \qquad \text{and} \qquad b'(x)\alpha(b(x)) = \alpha(x)\,. \tag{64}$$

Now assume that a, b are C^1-functions such that $a(x) < x < b(x)$ and $a = b^{-1}$. Let $\alpha : [0, b(0)] \to \mathbb{R}_+$ be a positive function such that

$$\int_{0}^{b(0)} \alpha(t)\,\mathrm{d}t = 1\,. \tag{65}$$

we extend α to $[a(0), 0[$ by letting $\alpha(x) = \alpha(b(x))\, b'(x)$ and to $]b(0), b(b(0))]$ by letting $\alpha(x) = \alpha(a(x))\, a'(x)$. Repeating this procedure we extend α to a map $\mathbb{R} \to \mathbb{R}_+$. For $x \in [0, b(0)]$ we now have

$$\int_{x}^{b(x)} \alpha(t)\,\mathrm{d}t = \int_{x}^{b(0)} \alpha(t)\,\mathrm{d}t + \int_{b(0)}^{b(x)} \alpha(t)\,\mathrm{d}t$$

substituting $t = b(s)$ in the second integral yields

$$\begin{aligned} &= \int_{x}^{b(0)} \alpha(t)\,\mathrm{d}t + \int_{0}^{x} \alpha(b(s))\, b'(s)\,\mathrm{d}s \\ &= \int_{x}^{b(0)} \alpha(t)\,\mathrm{d}t + \int_{0}^{x} \alpha(a(b(s)))\, a'(b(s))\, b'(s)\,\mathrm{d}s \\ &= \int_{x}^{b(0)} \alpha(t)\,\mathrm{d}t + \int_{0}^{x} \alpha(s)\,\mathrm{d}s = 1\,. \end{aligned}$$

Similarly we see that $\int_{a(x)}^{x} \alpha(t)\,\mathrm{d}t = 1$ and that it also holds for $x \in [a(0), 0[$ and more generally for $x \in [a^n(0), a^{n-1}(0)[$ and $x \in]b^{n-1}(0), b^n(0)]$, i.e., for all $x \in \mathbb{R}$. So in the one dimensional case we have a solution but it is far from unique, any function $\alpha : [0, b(0)] \to \mathbb{R}_+$ satisfying (65) gives a solution.

7 Conclusion and future work

We have presented a two stage process that provides us with new colour coordinates. As seen in Table 1 the Euclidean distance in these new colour spaces reflects human perception better than the existing standards. The new coordinates are given in terms of B-splines so evaluation of them are very fast.

Viewing the MacAdam ellipses as unit circles leads to a new and so far unstudied geometrical problem, where we can give the full answer in the simple one dimensional case.

The present work is certainly not the end of the story. I am convinced that step one in the algorithm, determing the Riemannian metric, can be improved and the different approaches mentioned in Section 1 should be tried. The construction should be carried out in the full 3D colour space taking all available data into account. Ideally the resulting colour differences should be validated by performing new experiments.

References

[1] ITU-R Recommendation BT. 709. *Basic Parameter Values for the HDTV Standard for the Studio and for the International Program Exchange*. ITU, 1211 Geneva 20, Switzerland, 1991.

[2] CIE colour matching functions. `http://cvrl.ioo.ucl.ac.uk/cmfs.htm`.

[3] CIE 116:1995 industrial colour-difference evaluation. Technical report, CIE, 1995.

[4] CIE 142:2001 Improvement to industrial colour-difference evaluation. Technical report, CIE, 2001.

[5] CIE 170-1:2006 Fundamental chromaticity diagram with physiological axes - part 1. Technical report, CIE, 2006. ISBN: 978 3 901906 46 6.

[6] H.J.A. Dartnell, J.K. Bowmaker, and J.D. Mollon. Human visual pigments: Microspectrophotometric results from the eyes of seven persons. *Proc. Royal Soc. London. Series B, Biological Sciences*, 220:115–130, 1983.

[7] J. Gravesen, A. Evgrafov, D.M. Nguyen, and P. Nørtoft. Planar parametrization in isogeometric analysis. In M. Floater, T. Lyche, M.-L. Mazure, K. Mørken, and L. Schumaker, editors, *Proceedings of the "Eighth International Conference on Mathematical Methods for Curves and Surfaces. Oslo, 2012*, volume 8177 of *Lecture Notes in Computer Science*, pages 189–212. Springer, 2014.

[8] I. Lissner and P. Urban. Toward a unified color space for perception-based image processing. *IEEE Transaction on Image Processing*, 21:1153–1168, 2012.

[9] D. L. MacAdam. Visual sensitivities to color differences in daylight. *J. Optical Soc. Amer.*, 32:247–274, 1942.

[10] MathWorks, Natick, Ma. *Matlab R2014b. Optimization Toolbox. User's Guide*, 2014.

[11] G. Sharma, W. Wu, and E.N. Dalai. The ciede2000 color-difference formula: Implementation notes, supplementary test data, and mathematical observations. *Color Research & Applications*, 30:21–30, 2004.

[12] Günter Wyszecki and W. S. Stiles. *Color Science, Concepts and Methods, Quantitative Data and Formulae*. John Wiley & Sons, New York, Chichester, Brisbane, Toronto, Singapore, 2. edition, 1982.